THE JOURNAL OF PHYSICAL CHEMISTRY A

Article

pubs.acs.org/JPCA

Quantification of the 248 nm Photolysis Products of HCNO (Fulminic Acid)

Wenhui Feng and John F. Hershberger*

Department of Chemistry and Biochemistry, North Dakota State University, Dept. 2735, P.O. Box 6050, Fargo, North Dakota 58108-6050, United States

ABSTRACT: IR diode laser spectroscopy was used to detect the products of HCNO (fulminic acid) photolysis at 248 nm. Five product channels are energetically possible at this photolysis wavelength: O + HCN, H + (NCO), CN + OH, CO + NH, and HNCO. In some experiments, isotopically labeled $^{18}O_2$, $^{15}N^{18}O$ and C_2D_6 reagents were included into the photolysis mixture in order to suppress and/or isotopically label possible secondary reactions. HCN, $OC^{18}O$, $C^{18}O$, NCO, DCN, and NH molecules were detected upon laser photolysis of HCNO/reagents/buffer gas mixtures. Analysis of the yields of product molecules leads to the following photolysis quantum yields: ϕ_{1a} (O + HCN) = 0.39 ± 0.07, ϕ_{1b} (H + (NCO)) = 0.21 ± 0.04, ϕ_{1c} (CN + OH) = 0.16 ± 0.04, ϕ_{1d} (CN + NH($a^1\Delta$)) = 0.19 ± 0.03, and ϕ_{1e} (HNCO) = 0.05 ± 0.02, respectively. The uncertainties include both random errors (1σ) and consideration of major sources of systematic error. In conjunction with the photolysis experiment, the H + HCNO reaction was investigated. Experimental data demonstrate that this reaction is very slow and does not contribute significantly to the secondary chemistry.

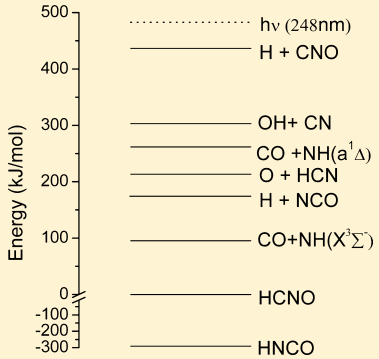

1. INTRODUCTION

Fulminic acid, HCNO, is an important intermediate in NO-reburning processes for reduction of NO_x pollutants from fossil-fuel combustion emission.[1] HCNO is formed in combustion primarily by the CH_2 + NO[2−5]and HCCO + NO[6−10] reactions. The chemistry of HCNO is therefore of great interest in the overall NO-reburning mechanism. In our laboratory, we have previously studied the kinetics of the OH + HCNO, CN + HCNO, NCO + HCNO and O + HCNO reactions,[11−15] using UV laser photolysis of precursor molecules at 248 nm or 266 nm to form the radical species (OH, CN, NCO, or O). In the course of these experiments, we observed significant yields of several product molecules in the absence of the precursor molecule, which was attributed to direct photolysis of HCNO. In those experiments, HCNO photolysis yields were treated as background signals that were generally subtracted from the product yields obtained in the presence of the radical precursor. In this study, we quantitatively examine the products produced by HCNO photolysis.

The ultraviolet absorption spectrum of HCNO was previously studied.[16] The observed spectrum was a single progression of vibronic bands over the range 244−285 nm. In addition, the UV photolysis of HCNO has previously been studied by Bondybey et al.[17] They used FTIR spectroscopy to observe HNCO as the primary final product. This molecule was assumed to be a result of secondary chemistry subsequent to the photolysis event. In the present study, time-resolved infrared laser spectroscopy is employed to detect the transient photolysis product signals to obtain a direct measurement of the major photolysis product channels. There are five energetically accessible channels at 248 nm:

$$\mathrm{HCNO} + h\nu(248\ \mathrm{nm}) \rightarrow \mathrm{O} + \mathrm{HCN} \quad (1a)$$

$$\rightarrow \mathrm{H} + (\mathrm{NCO}) \quad (1b)$$

$$\rightarrow \mathrm{OH} + \mathrm{CN} \quad (1c)$$

$$\rightarrow \mathrm{CO} + \mathrm{NH}(a^1\Delta) \quad (1d)$$

$$\rightarrow \mathrm{HNCO} \quad (1e)$$

NCO is written as (NCO) to indicate that we cannot distinguish between NCO and CNO isomers in this study. Figure 1 shows the energetics of these species. The thermochemical information has been obtained from standard tables[18] as well as other literature for the heats of formation of HCNO NCO[19] and NH ($a^1\Delta$).[20] Formation of ground state NH ($X\ ^3\Sigma^-$) is also possible, but is less likely as a spin-forbidden process.

2. EXPERIMENTAL SECTION

The photolysis laser was an excimer laser (Coherent, Compex-pro) operating at 248 nm. Reaction products were detected by infrared diode laser absorption spectroscopy. Several lead salt diode lasers (Laser Components) operating in the 80−110 K temperature range were used to provide tunable infrared probe laser light. The IR beam was collimated by a lens and combined with the UV light by means of a dichroic mirror, and both 0.6-cm diameter beams were copropagated though a 1.43 m absorption cell. After the UV light was removed by a second

Received: November 14, 2013
Revised: January 13, 2014
Published: January 24, 2014

ACS Publications © 2014 American Chemical Society

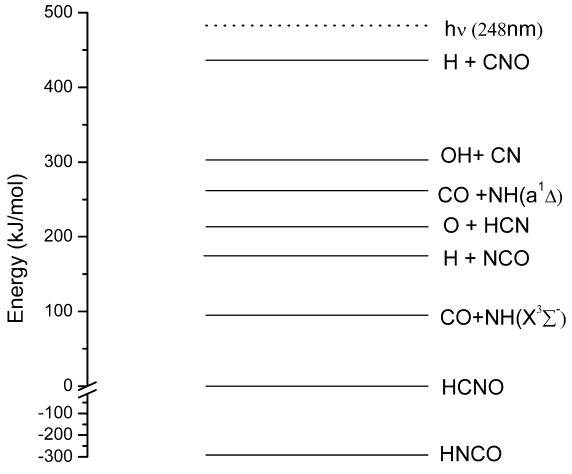

Figure 1. Relative Energy levels of possible photolysis products of HCNO photolysis. Thresholds (kJ/mol) compared to HCNO: −291.2 (HNCO), 95.1 (CO+NH (X $^3\Sigma^-$)), 174.5 (H+NCO), 213.3 (O +HCN), 261.9 (CO+ NH ($a^1\Delta$)), 303.1 (OH+CN), 436.6 (H +CNO). 248 nm photon provides 482.7 kJ/mol.

dichroic mirror, the infrared beam was then passed into a 1/4 m monochromator and focused onto a 1 mm InSb detector (Cincinnati Electronics, ∼1 μs response time). Transient infrared absorption signals were recorded on a digital oscilloscope (Lecroy, Wavesurfer 422) and transferred to a computer for analysis. All experiments were performed at 298 K.

HCNO samples were synthesized as previously described[20−23] by flash vacuum pyrolysis of 3-phenyl-4-oximino-isoxazol-5(4H)-one. The precursor (2.0 g) was sublimed from a 50 mL bulb in a 90 °C oil bath and passed through a horizontal quartz tube heated to 450 °C in a tube furnace. The products, which include HCNO, HNCO, CO_2, H_2O, and phenyl cyanide, were collected over a 48 h period at 77 K. H_2O and phenyl cyanide were removed by twice passing the products through a 240 K trap. CO_2 and HCNO were removed by vacuum distillation at 192 K. The purity of the HCNO samples was characterized by FT-IR spectroscopy via a strong absorption band at 2195 cm^{-1}.[24] The sample purity was estimated at 95% or better, with only small CO_2 and HNCO impurities. The HNCO impurity was monitored by FT-IR at a strong band at 2168 cm^{-1}.[25] Because HCNO has poor long-term stability, samples were kept at 77 K except when filling the reaction cell. In general, HCNO could be allowed to stand at room temperature for ∼5 min at below ∼0.5 Torr pressure in our Pyrex absorption cell with minimal decomposition.

HNCO was synthesized by the reaction of NaOCN (Aldrich 96%) with hydrogen chloride gas.[26] NaOCN was contained in a flask and evaluated. A measured pressure of HCl was filled into the NaOCN-containing flask and then frozen onto the NaOCN solid by immersing the flask into a liquid nitrogen bath. After several cycles of warming and freezing of the sample, the reaction products were purified by distillation at −193 K to remove trace HCl and CO_2.

Hydrazoic acid (HN_3) was synthesized by melting stearic acid (Aldrich) over sodium azide (Aldrich) at 343 K and purified by freeze−pump−thaw cycles at 193 K to remove N_2O. Purity was checked by measurement of the UV absorption coefficient and comparison with literature values.

SF_6 and CF_4 (Matheson) was purified by repeated freeze−pump−thaw cycles at 77 K and by passing through an Ascarite II column to remove traces of CO_2. $^{15}N^{18}O$ (Isotec) was purified by repeated freeze−pump−thaw cycles at 153 K. The following molecules were probed using infrared diode laser absorption spectroscopy:

HCN ($v = 1 \leftarrow v = 0$) P(17) at 3258.441 cm^{-1}

DCN ($v = 1 \leftarrow v = 0$) R(7) at 2648.9 cm^{-1}

$OC^{18}O$ ($\nu 1$, $v = 1 \leftarrow v = 0$) P(15) at 2320.46 cm^{-1}

CO ($v = 1 \leftarrow v = 0$) R(13) at 2193.359 cm^{-1}

$C^{18}O$ ($v = 1 \leftarrow v = 0$) R(15) at 2146.198 cm^{-1}

NCO ($v = 1 \leftarrow v = 0$) at 1904.14 cm^{-1}

NH ($v = 1 \leftarrow v = 0$) R(3) 3242.89 cm^{-1}

HNCO ($v = 1 \leftarrow v = 0$) (R10) 2276.71 cm^{-1}

The HITRAN molecular database was used to locate and identify the spectral lines of CO, $C^{18}O$, $OC^{18}O$, and HCN product molecules.[27] Other published spectral data were used to locate and identify DCN,[28] NCO,[29] NH[30] and HNCO[25] lines.

Typical experimental conditions were P(HCNO) = 0.1 Torr, $P(^{15}N^{18}O)$ = 1.0 Torr, $P(^{18}O_2)$ = 1.0−4.0 Torr, P(SF_6 or CF_4) = 1.50 Torr, $P(C_2D_6)$ = 0.5−7.0 Torr, P(Xe) = 2.0 Torr, and 248 nm laser pulse energies of 25 mJ (fluence of ∼88 mJ/cm^2).

3. RESULTS

Infrared diode laser absorption was used to detect product molecules (or products of secondary chemistry) from channels 1a−1e upon 248 nm laser photolysis of HCNO/buffer gas. In order to modify and/or suppress potential secondary chemistry, additional reagents were sometimes included in the reaction mixture, as described below. Figure 2 shows some typical signals for detection of HCN, CO, and CO_2 molecules. Typically, transient signals show a fast (∼10−100 μs) rise, followed by a slow (∼1 ms) decay. The rise is attributed to formation of the detected product by either direct photolysis and/or subsequent secondary chemistry, as described below. The decay is attributed to diffusion of molecules out of the probed volume. The rate of the rise is primarily determined by the rate of collisional relaxation of a nascent vibrational distribution to a Boltzmann distribution. The choice of buffer gas (SF_6 for detection of most molecules, but CF_4 for detection of CO molecules)[31,32] was motivated by the desire to maximize this relaxation rate, while keeping the total pressure sufficiently low to minimize pressure broadening of spectral lines.

In order to estimate the yields, the slow decay portion of each transient signal was fit to a single exponential decay (diffusion out of a cylindrical volume is not strictly exponential, but this is sufficient for our purpose). Transient signal amplitudes were obtained by extrapolation to t = 0 (this extrapolated amplitude was typically a small (∼5−15%) increase compared to the peak−peak amplitudes). The resulting amplitudes were converted into absolute concentrations using HITRAN line strengths for all of the detected molecules except for NH radicals and DCN molecules, which were calibrated as described below. Table 1 shows the resulting yields of the detected molecules.

dx.doi.org/10.1021/jp411209n | J. Phys. Chem. A 2014, 118, 829−837

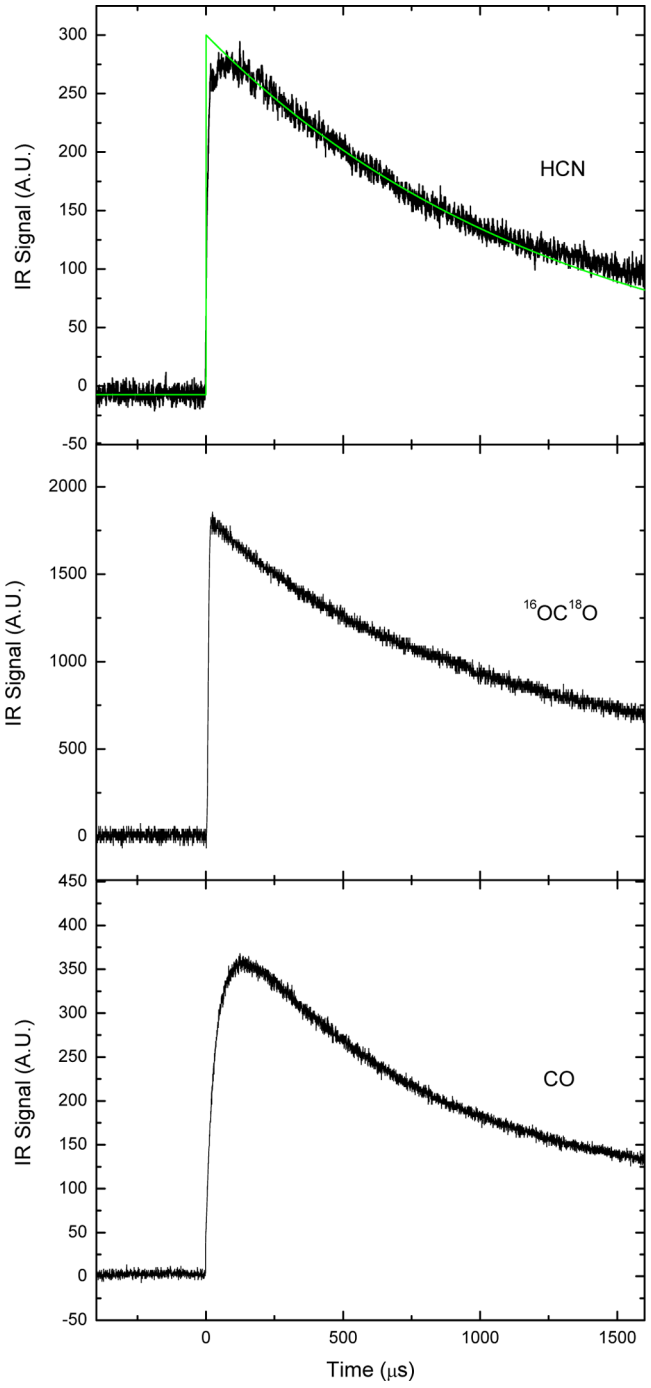

Figure 2. Transient signals of HCN (top panel) and $^{16}OC^{18}O$ (middle panel) detected upon laser photolysis of HCNO(0.1 Torr)/$^{15}N^{18}O$ (1 Torr)/SF_6 (1.5 Torr) mixture, and CO (bottom panel) detected upon photolysis of HCNO(0.1 Torr)/$^{18}O_2$ (1.0 Torr) /CF_4 (1.5 Torr) mixture. 248 nm photolysis laser pulse energy = 25 mJ. Green curve in top panel shows a typical single exponential fit to the decay portion of the signal.

Our previous studies show that HCNO is a highly reactive molecule. Many secondary reactions following the photolysis must therefore be considered:

$$O + HCNO \rightarrow H + CO + NO \quad (2)$$

$$CN + HCNO \rightarrow NO + HCCN \quad (3)$$

$$NCO + HCNO \rightarrow HCN + CO + NO \quad (4)$$

Table 1. Yields of Products of HCNO Photolysis and Secondary Reactions[a]

product	yield (10^{12} molecules cm^{-3})
HCN	20.0 ± 1
$OC^{18}O$	6.0 ± 0.3
$C^{18}O$	15 ± 2
DCN	8.3 ± 0.9
CO	19.5 ± 2
NH	9.7 ± 1
HNCO	2.5 ± 0.2

[a]Experimental conditions: P(HCNO) = 0.1 Torr, $P(^{15}N^{18}O)$ = 1.5 Torr, $P(^{18}O_2)$ = 1.0–4.0 Torr, $P(CF_4)$ = 1.5 Torr (CO detection only), $P(SF_6)$ = 1.5 Torr (HCN, NCO, DCN and CO detection), 248 nm photolysis laser pulse energy ~25 mJ. Uncertainties represent one standard deviation.

$$OH + HCNO \rightarrow CO + H_2NO \quad (5a)$$

$$\rightarrow HCO + HNO \quad (5b)$$

$$\rightarrow NO + H_2CO \quad (5c)$$

$$NH + HCNO \rightarrow \text{products} \quad (6)$$

$$H + HCNO \rightarrow \text{products} \quad (7)$$

Reactions 2–6 have been studied previously in our lab,[11−15] resulting in the following rate constants: $k_2 = (5.32 \pm 0.4) \times 10^{-12}$ cm^3 $molecule^{-1}$ s^{-1}, $k_3 = (1.04 \pm 0.1) \times 10^{-10}$ cm^3 $molecule^{-1}$ s^{-1}, $k_4 = (1.58 \pm 0.2) \times 10^{-11}$ cm^3 $molecule^{-1}s^{-1}$, $k_5 = (3.4 \pm 0.3) \times 10^{-11}$ cm^3 $molecule^{-1}$ s^{-1} and $k_6 \leq 2.1 \times 10^{-13}$ cm^3 $molecule^{-1}$ s^{-1} at 298 K. As can be seen, reactions 2–5 are fast and produce some of the same molecules as direct photolysis, complicating the interpretation of product yields. The approach used here is to include additional reagents in the reaction mixture in order to suppress or redirect these secondary reactions, as described in detail below.

3.1. Product Channel 1a, O + HCN. In order to quantify the yield of channel 1a, (O + HCN), we detected the HCN product. If photolysis channel 1b is significant, however, additional HCN may be produced by reaction 4. Isotopically labeled $^{15}N^{18}O$ reagent was therefore included in the reaction mixture in order to suppress reaction 4:

$$NCO + {}^{15}N^{18}O \rightarrow N^{15}N^{18}O + CO \quad (8a)$$

$$\rightarrow N^{15}N + OC^{18}O \quad (8b)$$

(Product branching ratios at 296 K: $\varphi_{8a} = 0.44 \pm 0.07$; $\varphi_{8b} = 0.56 \pm 0.07$).[32] By comparing the rate constants $k_4 = (1.58 \pm 0.2) \times 10^{-11}$ cm^3 $molecule^{-1}$ s^{-1} and $k_8 = (4.3 \pm 0.4)$ x10^{-11} cm^3 $molecule^{-1}$ s^{-1},[33] we conclude that a 10:1 ratio of $^{15}N^{18}O$ to HCNO pressure is sufficient to ensure that nearly all NCO radicals react by reaction 8 rather than 4, and therefore do not result in HCN production.

We note that if channel 1c is significant, the resulting CN radicals will still react primarily with HCNO (reaction 3), since the CN + NO reaction is slow at the low pressures used here. Reaction 3 produces HCCN radicals,[12,15] which further react with $^{15}N^{18}O$ to produce isotopically labeled HCN:

$$CN + HCNO \rightarrow NO + HCCN \quad (3)$$

$$HCCN + {}^{15}N^{18}O \rightarrow HC^{15}N + NC^{18}O \quad (9)$$

Our experiment, however, detects the nonlabeled $HC^{14}N$ isotope, and is therefore not affected by this secondary

dx.doi.org/10.1021/jp411209n | J. Phys. Chem. A 2014, 118, 829–837

chemistry. The nitrogen-15 labeling is therefore crucial for this experiment (the oxygen-18 labeling is not).

Other potential secondary reactions include O + HCNO, OH + HCNO, NH + NO, NH + HCNO, etc. To the best of our knowledge, however, these reactions do not produce HCN. Therefore, the HCN signal obtained upon photolysis of a HCNO(0.1 Torr)/$^{15}N^{18}O$ (1 Torr) /SF_6 (1.5 Torr) mixture, as shown in Figure 2, can be attributed to photolysis channel 1a.

3.2. Product Channel 1b, H + (NCO). In order to quantify the yield of channel 1b, H + (NCO), several approaches are possible. One is direct detection of NCO molecules upon photolysis of a HCNO(0.1 Torr)/SF_6 (1.5 Torr) mixture, as shown in Figure 3. The NCO transient signal shows a ~ 50 μs

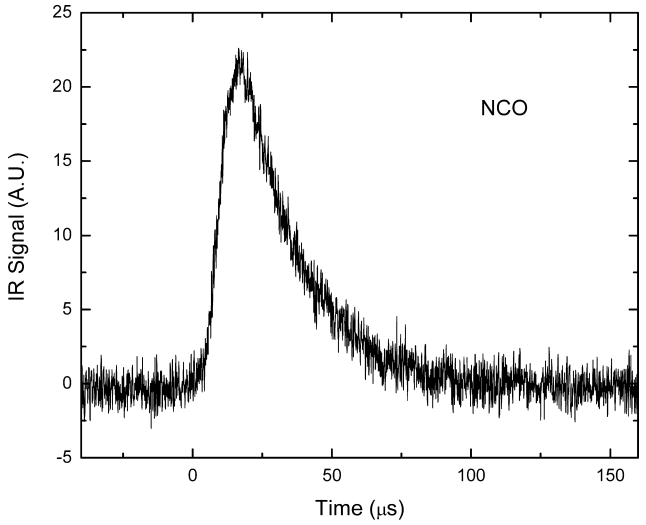

Figure 3. Transient signal of NCO detected upon photolysis of HCNO(0.2Torr)/SF_6(1.5 Torr) mixture and 248 nm photolysis; laser pulse energy ~25 mJ.

fast decay lifetime due to its reaction with HCNO. Although this provides evidence for the existence of channel 1b, we have not measured the infrared absorption coefficients of NCO needed to quantify yields. Instead, we added isotopically labeled $^{15}N^{18}O$ reagent in the photolysis mixture as described above in order to initiate reaction 8. Under these conditions, $OC^{18}O$ is produced in reaction 8b, as shown in Figure 2. Unlike NCO, we do have absorption coefficients for $OC^{18}O$ from the HITRAN database, allowing quantification (although the HITRAN line strengths must be divided by the O-18 natural isotopic abundance to account for the fact that HITRAN assumes natural abundance, unlike our enriched sample). Therefore, assuming we have an excess of $^{15}N^{18}O$ which results in all NCO radicals reacting via eq 8, and knowing the branching ratio into 8b, we quantify the yield of NCO molecules originally produced in photolysis channel 1b:

$$[NCO]_{1b} = [OC^{18}O]/0.56$$

We assume here that the isotopic substitution does not affect the branching ratio. Additional secondary chemistry can possibly produce CO_2, as follows:

$$CN + HCNO \rightarrow NO + HCCN \quad (3)$$

$$HCCN + {}^{15}N^{18}O \rightarrow HC^{15}N + NC^{18}O \quad (9)$$

$$NC^{18}O + {}^{15}N^{18}O \rightarrow N^{15}N + {}^{18}OC^{18}O \quad (8b^*)$$

Here, the notation 8b* is used to identify an isotopic variant of reaction 8b. As can be seen, the carbon dioxide molecules in reaction 8b* are double labeled ($^{18}OC^{18}O$) and do not contribute to the yield of the singly labeled $OC^{18}O$, and therefore do not interfere with this measurement.

We should note here that we have no method to detect CNO, a high energy isomer of NCO. It is likely that any CNO formed quickly isomerizes to NCO. Our experiment is unable to distinguish whether this would happen during the photolysis process or subsequent to fragmentation. In any case, our measurement of the yield of channel 1b should be considered the sum of H + CNO and H + NCO photolysis events.

3.3. Product Channel 1c, CN + OH. In order to detect the presence of photolysis channel 1c, CN + OH, we attempted to directly detect CN radicals. This was not successful, possibly because CN is very rapidly depleted by the extremely fast reaction 3. In principle, one could attempt to quantify this channel by detection of NO molecules produced in reaction 3, but this approach is complicated by other secondary chemistry such as O + HCNO, reaction 2, which also produces NO. We therefore used two alternative approaches.

The first approach was to add $^{18}O_2$ reagent to the photolysis mixture in order to initiate the following reaction sequence:

$$CN + {}^{18}O_2 \rightarrow NC^{18}O + {}^{18}O \quad (10a)$$

$$\rightarrow N^{18}O + C^{18}O \quad (10b)$$

$$NC^{18}O + HCNO \rightarrow HCN + NO + C^{18}O \quad (4^*)$$

$$^{18}O + HCNO \rightarrow H + NO + C^{18}O \quad (2^*)$$

As described above, the asterisk notations in the reaction numbering denote an isotopic variant. If channel 1c is significant, we expect $C^{18}O$ in reactions 10, 4* and 2* to be detected upon photolysis of an HCNO(0.1 Torr)/$^{18}O_2$ (4.0 Torr)/CF_4 (1.5 Torr) mixture. Figure 4 shows the resulting signal. Reaction 10 has a rate constant of $k_{10} = 2.3 \times 10^{-11}$ cm^3 molecule^{-1} s^{-1} at 298 K[34] and a branching ratio of $\varphi_{10a} = 0.8$ and $\varphi_{10b} = 0.2$.[35] As other secondary reactions, for instance (H, O, NCO, NH or OH) + $^{18}O_2$, OH + HCNO, etc., do not produce $C^{18}O$, we can estimate that each CN molecule produces 0.8 NCO molecules and 0.8 O molecules by reaction 10a; the former produces 0.8 $C^{18}O$ by reaction 4*, and the latter produces another 0.8 $C^{18}O$ by reaction 2*. Adding the 0.2 $C^{18}O$ from reaction 10b, we estimate a total of 1.8 $C^{18}O$ molecules should be produced from one CN molecules. Therefore, the yield of photolysis channel 1c is $[CN] = [C^{18}O]/1.8$. In order for this to work, an overwhelming amount of $^{18}O_2$ must be used in order to suppress the competing reaction CN + HCNO. At $[^{18}O_2] = 4.0$ Torr, about 90% of CN + HCNO reaction will be suppressed. Table 1 shows the measured concentration of $C^{18}O$ is $(1.5 \pm 0.2) \times 10^{13}$ molecules cm^{-3}, from which we obtain $[CN] = (8.3 \pm 1.0) \times 10^{12}$ molecules cm^{-3}. There is one disadvantage of this method. Among reactions 2−5, the O + HCNO reaction is relatively slow, and it is not clear that all of the O atoms react with HCNO under our conditions.

The second approach to determining the yield of photolysis channel 1c is to add deuterated ethane, C_2D_6, resulting in the secondary reaction to produce DCN:

$$CN + C_2D_6 \rightarrow C_2D_5 + DCN \quad (11)$$

dx.doi.org/10.1021/jp411209n | J. Phys. Chem. A 2014, 118, 829−837

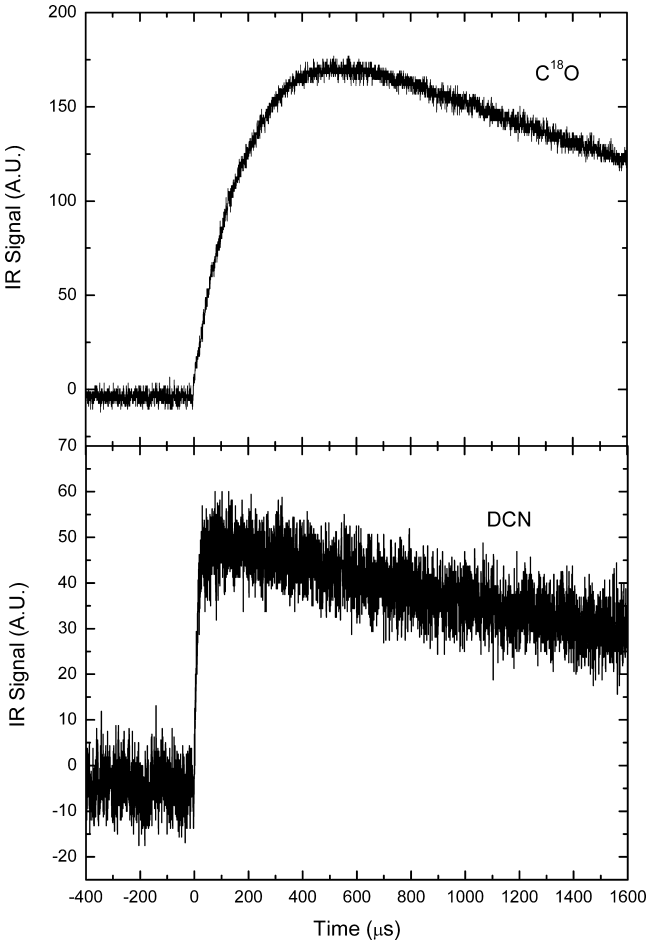

Figure 4. Transient signal of $C^{18}O$ and DCN detected upon photolysis of HCNO(0.1 Torr)/$^{18}O_2$ (4.0 Torr)/CF_4 (1.5 Torr) mixture and HCNO(0.1Torr)/ C_2D_6 (5.0 Torr)/SF_6 (1.5 Torr) mixture, respectively. 248 nm photolysis laser pulse energy ~25 mJ.

Figure 4 shows the resulting signals. We measured the DCN signal as a function of C_2D_6 pressure upon photolysis of HCNO(0.1Torr)/C_2D_6 (variable: 0.5−7.0 Torr)/SF_6 (1.5 Torr) mixtures. These data, after calibration, are shown in Figure 5.

Literature line strengths for DCN are not available, so we calibrated the DCN signals as follows: several DCN transient signals were detected upon 248 nm laser photolysis of an ICN (0.05−0.15Torr)/C_2D_6 (1.0 Torr)/SF_6 (1.5 Torr) mixture. Under these conditions, CN is produced by photolysis of ICN, and most of the CN molecules react to form DCN, so the concentration of DCN is expected to be equal to that of CN. The latter was calculated using the 248 nm absorption coefficient of ICN (α = 0.009 $Torr^{-1}cm^{-1}$) and a quantum yield of unity and measurement of the photolysis laser energy. From the plot of DCN IR absorptions as the functions of DCN concentrations, we can obtain the infrared absorption coefficient of the probed DCN line under low pressure (<2 Torr) conditions. One additional correction must be mentioned, however. Because Figure 5 extends to substantially greater pressures than the 1−2 Torr values typical in our experiments, pressure broadening effects may substantially reduce the DCN absorption coefficients below those determined at low pressures. Literature values of pressure broadening coefficients are not available for this specific

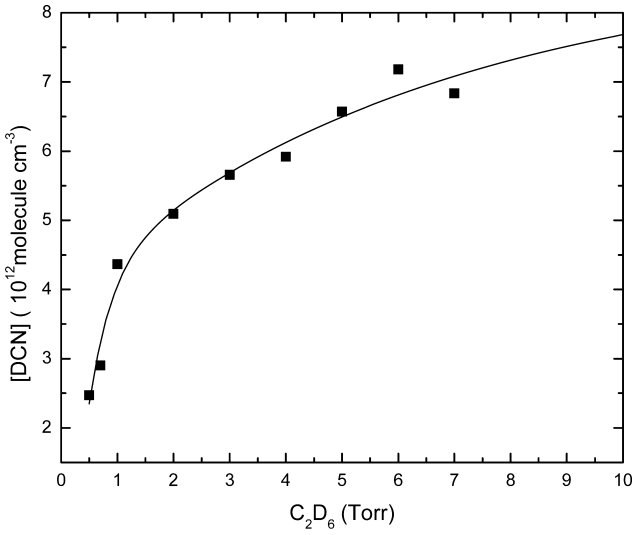

Figure 5. The yields of DCN as the function C_2D_6 pressures. DCN was detected upon photolysis of HCNO(0.1Torr)/C_2D_6(variable: 0−7.0 Torr)/SF_6(1.5 Torr) mixture; 248 nm photolysis laser pulse energy ~25 mJ. The experimental data was simulated by the function: $y = -2.40\exp(-x/6.44) - 2.40\exp(-x/6.45) - 6.82\exp(-x/0.39) + 8.7$.

combination of gases, so this effect was estimated by measuring the absorption at line center of static DCN samples as a function of added C_2D_6, as shown in Figure 6. As can be seen,

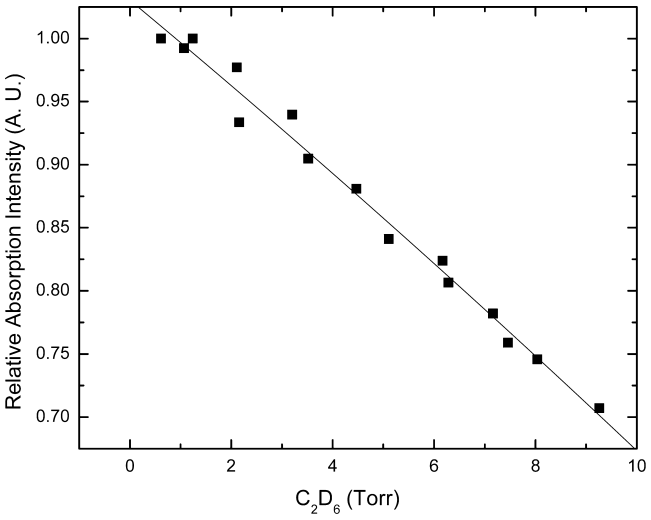

Figure 6. The relative IR absorption intensities at the center of the DCN R(7) line as the function of the pressure of C_2D_6.

pressure broadening results in a ~25−30% decrease in absorption at the higher pressures (7−10 Torr) used. This is somewhat larger than typical pressure broadening affects. The data in Figure 5 was therefore corrected for pressure broadening, a modest but significant (~25%) correction.

As shown in Figure 5, the DCN yield has not completely peaked even at the highest C_2D_6 pressures used. This is consistent with the kinetics involved: the rate constant of reaction 11 was measured in our lab to be $k_{11} \sim 1.2 \times 10^{-11}$ cm^3 $molecule^{-1}cm^{-1}$. (This is about four times slower than that of the CN + C_2H_6 reaction, a reasonable kinetic isotope effect). Using our value of k_{11} and k_3, we estimate that about 10 Torr C_2D_6 (versus 0.1 Torr HCNO) is needed to suppress

dx.doi.org/10.1021/jp411209n | J. Phys. Chem. A 2014, 118, 829−837

most of the competing CN + HCNO reaction. In order to estimate the DCN yield expected at 20 Torr C_2D_6, where reaction 3 should be completely suppressed, the data was simulated by using a three parameter exponential equation, as shown in Figure 5. Using this simulation equation, we estimated the [DCN] = 8.26 × 10^{12} molecules cm^{-3} at $[C_2D_6]$ = 20 Torr, which, by comparison, is very close to the [CN] value obtained by the first approach (involving $^{18}O_2$, described above). We therefore estimate the yield of channel 1c to be [CN] = (8.3 ± 0.9) × 10^{12} molecules cm^{-3}. This result is shown in Table 2.

Table 2. Yields of Products of HCNO Photolysis[a]

product	yield (10^{12} molecules cm^{-3})
HCN	20.0 ± 1
NCO	10.7 ± 0.5
CN	8.3 ± 0.9
NH	9.7 ± 1
HNCO	2.5 ± 0.5
Total	51.2

[a]Experimental conditions: P(HCNO) = 0.1 Torr, P(CF_4 or SF_6) = 1.5 Torr, and 248 nm photolysis laser pulse energy ~25 mJ. Uncertainties represent one standard deviation.

3.4. Product Channel 1d, CO + NH. We have also attempted to quantify the yield of channel 1d, by detecting CO product molecules. Unfortunately, multiple secondary reactions can contribute to the CO yield, including O + HCNO, NCO + HCNO, and OH + HCNO reactions. Reaction 5, OH + HCNO reaction has product branching ratios of φ_{5a} = 0.61, φ_{5b} = 0.35 and φ_{5c} = 0.04.[11] The HCO product in 5b could possibly dissociate to H + CO to add more CO molecules. In order to simplify the analysis, we included isotope labeled $^{18}O_2$ in the photolysis mixture, but still detected the unlabeled $C^{16}O$ product, obtaining the signal shown in Figure 2 (bottom panel). This removes some but not all of the secondary chemistry: any CN produced in 1c will react with $^{18}O_2$ to form ^{18}O and/or $NC^{18}O$. These species, when reacted with HCNO, will probably make $C^{18}O$ rather than the detected $C^{16}O$. Nevertheless, substantial secondary chemistry remains: any HCO produced in 5b reacts as follows:

$$HCO + {}^{18}O_2 \rightarrow CO + H^{18}O_2 \quad (12)$$

Therefore one OH molecule is estimated to form 0.96 CO molecules (the sum of φ_{5a} and φ_{5b}). In addition, any O atoms formed in 1a or NCO radicals formed in 1b will react, producing additional CO. We can very roughly estimate

$$[CO]_{1d} = [CO]_{total} - [CO]_{O+HCNO} - [CO]_{NCO+HCNO} - [CO]_{OH+HCNO}$$

$$[CO]_{O+HCNO} = [O]_{1a} = [HCN]_{1a}$$

$$[CO]_{NCO+HCNO} = [NCO]_{1b}$$

$$[CO]_{OH+HCNO} = [OH]_{1c} = [CN]_{1c} \times 0.96$$

The $[CO]_{total}$ denotes the total CO concentration detected upon laser photolysis of HCNO(0.1 Torr)/$^{18}O_2$(1.0 Torr)/CF_4(1.5 Torr) mixture, as shown in Table 1. Unfortunately, this calculation results in a negative value for $[CO]_{1d}$, indicating that some of our assumptions are unfounded. For example, it is likely that not all of the O atoms formed in 1a react with HCNO, as k_2 is quite small, and diffusional loss likely competes for O atoms. If one assumes that only half of the O atoms react via reaction2, one obtains $[CO]_{1d} \sim 0$. Based on the large uncertainties in the secondary chemistry, we conclude that detection of CO is not a very good method to quantify the yield of channel 1d.

Another possible approach to quantifying channel 1d is direct detection of the NH radical. We have successfully detected the NH($X\ ^3\Sigma^-$) radical upon photolysis of HCNO(0.1Torr)/Xe (2.0 Torr)/SF_6 (2.0 Torr) mixture, as shown in Figure 7.

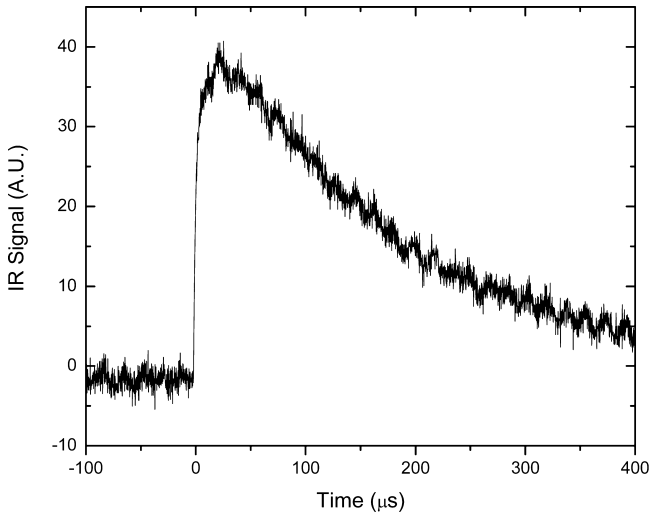

Figure 7. Transient signal of NH radical detected upon photolysis of HCNO(0.1Torr)/Xe(2.0 Torr)/SF_6(2.0 Torr) mixture and 248 nm photolysis, laser pulse energy ~25 mJ.

Xenon gas was used to relax electronic excited state NH($a^1\Delta$) to ground state NH($X\ ^3\Sigma^-$).[36,37] No NH($X\ ^3\Sigma^-$) signal was detected in the absence of xenon, suggesting that direct photolysis of HCNO produces NH exclusively in the excited ($a^1\Delta$) state. There is no IR absorption line strength of NH was reported, so we measured it by the following experiment. NH transient signal was detected upon photolysis of HN_3 (variable: 0.1−0.4 Torr)/Xe (2.0 Torr)/SF_6 (2.0 Torr) mixtures. Hydrazoic acid (HN_3) photolysis produces NH($a^1\Delta$):

$$HN_3 + h\nu(248nm) \rightarrow NH(a^1\Delta) + N_2 \quad (13a)$$

$$\rightarrow H + N_3 \quad (13b)$$

(The photolysis quantum yields are φ_{13a} = 0.76; φ_{13b} = 0.24).[38] The NH concentration in our experiment was estimated from the 248 nm absorption coefficient of HN_3 (α = 0.0022 $Torr^{-1}cm^{-1}$) and a quantum yield of 0.76 and measurement of the photolysis laser energy. From the slope of a plot of $\ln(I/I_0)$ as a function of NH concentration, we obtain the NH absorption cross section of 6.57 × 10^{-18} cm^2 $molecule^{-1}$ for the R(10) line, and use it to convert the absorption amplitude of the detected NH signal to number density to be (9.7 ± 1) × 10^{12} cm^3.

Other possible approaches to quantifying channel 1d, involving N_2O detection from the NH + NO reaction were considered, but were rejected because they also had large amounts of competing secondary chemistry.

3.5. Product Channel 1e, HNCO. The HNCO photolysis product was detected upon laser photolysis of an HCNO(0.1

dx.doi.org/10.1021/jp411209n | J. Phys. Chem. A 2014, 118, 829−837

Torr)/SF_6(1.0 Torr) mixture using an HNCO R(10) absorption line at 2276.71 cm^{-1}. The IR absorption cross section at line center was measured to be 4.75×10^{-17} cm^2 $molecule^{-1}$ by measurement of the absorption of static samples of HNCO. One difficulty is that our HCNO samples have a small level of HNCO impurity, typically a few percent. This amount is sufficient to substantially interfere with detection of HNCO transient signals. Therefore, for the HNCO detection experiments, additional purification of the HCNO sample was conducted to reduce the HNCO impurity to ~0.2%; this resulted in about ~3% absorption of the infrared light at the HNCO R(10) line. Although still not ideal, slow dark reactions that convert HCNO to HNCO prevented better purification.

Figure 8a shows the HNCO transient signal obtained from the photolysis of HCNO(0.1 Torr)/SF_6(1.0 Torr). Before attributing the signal to photolysis channel 1e, we must consider the possibility that some of the secondary chemistry, reactions 2−5, may result in collision-induced isomerization of HCNO to HNCO. Ab initio studies of the potential energy surface studies of these reactions[39−44] do not show any low energy pathways leading to HNCO, and the previous experimental observations of fast radical decay suggest that isomerization does not play a major role, but we cannot rule out a small contribution. Therefore, we included the reagents NO, NO_2, and O_2 in the reaction mixture in order to quench these radicals:

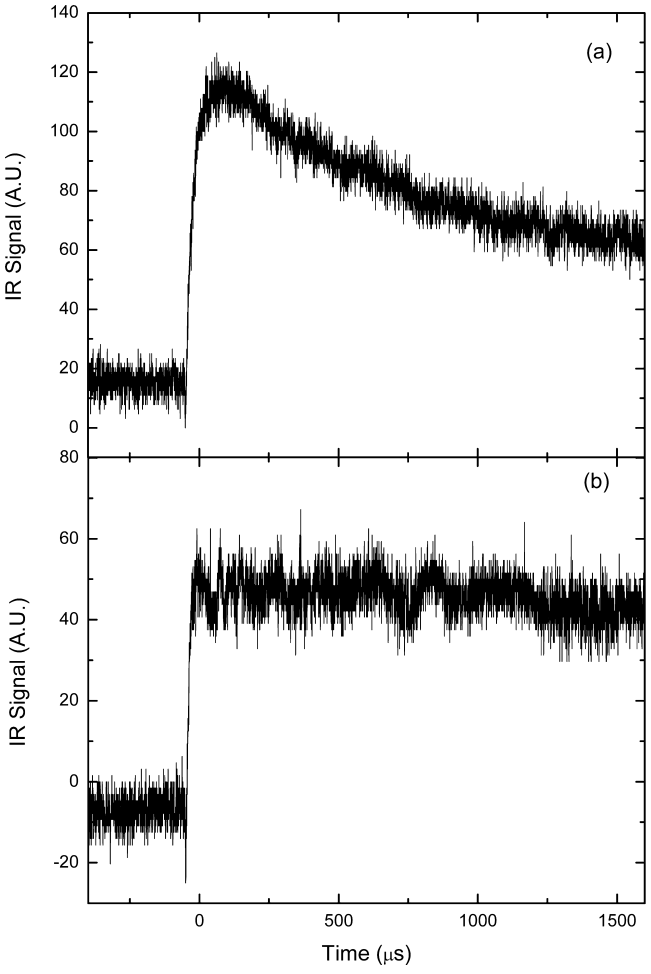

Figure 8. The HNCO transient IR absorption signal detected upon photolysis of mixture (a) HCNO (0.1 Torr)/SF_6(1.5 Torr) and (b) HCNO(0.1Torr)/NO(1.0 Torr)/NO_2(1.0 Torr)/O_2(4.0 Torr)/SF_6(1.5 Torr) using R10 line of HNCO.

$$CN + O_2 \rightarrow NCO + O \quad (10)$$

$$NCO + NO \rightarrow \text{products} \quad (8)$$

$$O + NO_2 \rightarrow NO + O_2 \quad (14)$$

As shown in Figure 8b, a smaller but still significant HNCO transient absorption signal was detected upon photolysis of a HCNO(0.1 Torr)/SF_6(1.0 Torr)/O_2(4.0 Torr)/NO(1.0 Torr)/NO_2(1.0 Torr) mixture. The slower decay in Figure (8b) compared to Figure (8a) is due to the greater total pressure, resulting in slower diffusional loss. Unfortunately, at least one of these reagents, probably NO_2, apparently reacts slowly with HCNO, resulting in an increase in the static HNCO impurity by a factor of ~2. We therefore believe that this signal is less reliable, and have chosen to use the signal from Figure 8a to quantify channel 1e. Although this results in substantial uncertainty, we do conclude that there is a small but nonzero yield of HNCO produced through the photoisomerization channel 1e.

3.6. Summary of Quantum Yields. Table 2 shows the resulting yields of the five HCNO photolysis channels after the above analysis to account for secondary chemistry. The sum of the channels gives a total product yield of $(5.12 \pm 0.39) \times 10^{13}$ molecules cm^{-3}. Assuming no other product channels, we calculate the product branching ratios to be (39.1 ± 2)%, (20.9 ± 1)%, (16.2 ± 2)%, (18.9 ± 2)%, and (4.8 ± 1)% for channels 1a, 1b, 1c, 1d, and 1e, respectively, where the uncertainties are random errors (one standard deviation).

Next we converted the product yields into photolysis quantum yields. We are not aware of any literature information on UV absorption cross sections. We therefore measured the UV absorption coefficient of HCNO at 248 nm by measuring the transmitted excimer laser energy as a function of HCNO pressure, and making a standard Beer−Lambert plot. We obtain $\alpha_{248} = (4.93 \pm 0.50) \times 10^{-3}$ $Torr^{-1}$ cm^{-1}, equivalent to a cross section of $\sigma_{248} = (1.52 \pm 0.15) \times 10^{-19}$ cm^2 $molecule^{-1}$. Although not used in the present study, we also measured absorption coefficients at other common photolysis wavelengths: $\alpha_{193} = 1.75\times 10^{-2}$ $Torr^{-1}$ cm^{-1} (or $\sigma_{193} = 5.39 \times 10^{-19}$ cm^2 $molecule^{-1}$), and $\alpha_{266} = 4.59\times 10^{-3}$ $Torr^{-1}$ cm^{-1} (or $\sigma_{266} = 1.42 \times 10^{-19}$ cm^2 $molecule^{-1}$). Using the absorption coefficient of HCNO at 248 nm and the photolysis laser energy (25 mJ/pulse) we estimated the number density of absorbed photons upon photolysis of 0.1 Torr HCNO at 248 nm to be $(5.14 \pm 0.40) \times 10^{13}$ cm^{-3}. Comparing with the product yield of channels 1a−1e, we can obtain photolysis quantum yields of $\phi_{1a} = 0.39 \pm 0.07$, $\phi_{1b} = 0.21 \pm 0.04$, $\phi_{1c} = 0.16 \pm 0.04$, $\phi_{1d} = 0.19 \pm 0.03$, and $\phi_{1e} = 0.05 \pm 0.02$. The sum of these quantum yields is unity, 1.00 ± 0.08, indicating that these experiments account for all of the major photolysis channels (the exact agreement with unity is probably fortuitous). The quoted uncertainties are obtained by propagation of the random errors inherent in the measurements as well as consideration of systematic errors due to estimated uncertainties in the infrared line strengths (typically ~5−10%), the UV laser energy (~5%), and the HCNO UV absorption coefficient (~10%).

One last issue concerns the fate of H atoms produced in channel 1b. If H atoms react quickly with HCNO (reaction 7), additional routes to some of the product molecules detected

dx.doi.org/10.1021/jp411209n | J. Phys. Chem. A 2014, 118, 829−837

may exist. No experimental measurement of k_7 has been reported, but there are two computational studies in the literature. A potential energy surface study by Wang et al. shows only one kinetically allowed product channel: HCN + OH,[45] and suggests that this is a fast reaction. If true, our interpretation of the HCN yield experiments are clearly in error. A theoretical calculation by Miller et al.,[1] however, shows this reaction is slow with a rate constant of $k = 1.2 \times 10^{-13}$ cm ^{3} s^{-1} $molec^{-1}$. If this is true, most H atoms would be lost to diffusional decay under our experimental conditions rather than react with HCNO. We do not have any way to directly detect H atoms, but we have investigated possible products:

$$H + HCNO \rightarrow CO + NH_2 \quad (7a)$$

$$\rightarrow CN + H_2O \quad (7b)$$

$$\rightarrow HCN + OH \quad (7c)$$

$$\rightarrow H_2CO + N \quad (7d)$$

In this experiment, H_2S precursor molecules were used to produce H atoms:

$$H_2S + h\nu\ (248nm) \rightarrow H + HS \quad (15)$$

We then attempted to detect HCN products upon 248 nm photolysis of an H_2S(0.2 Torr)/HCNO(0.2 Torr)/SF_6(1.0 Torr) mixture. Under experimental conditions of 25 mJ of laser energy, the expected concentration of H atoms produced from photolysis of 0.2 Torr H_2S was estimated to be [H] = 2.0×10^{13} cm^{-3} using the absorption coefficient of H_2S ($\alpha = 9.0 \times 10^{-4}$ $Torr^{-1}$ cm^{-1} at 248 nm[46] and assuming an H atom quantum yield of unity). This estimation was approximately confirmed by an experiment: we measured $\sim 2.0 \times 10^{13}$ cm^{-3} of NO molecules upon 248 nm laser photolysis of H_2S(0.2 Torr)/NO_2(0.2 Torr)/SF_6(1.0 Torr) mixture due to the following reactions:

$$H_2S + h\nu\ (248nm) \rightarrow H + HS \quad (15)$$

$$H + NO_2 \rightarrow NO + HO \quad (16)$$

Overall, the calculation and experiment shows that photolysis of 0.2 Torr H_2S at 248 nm can produce $\sim 2.0 \times 10^{13}$ cm^{-3} H atoms, which is comparable with the HCN yield from photolysis of HCNO. If there is HCN produced form reaction 7c, it should be measurable against the HCN background due to HCNO photolysis. Experimentally, we observe an HCN yield that is unchanged by the addition or omission of H_2S. This strongly suggests either that reaction 7 is slow or that channel 7c is not significant. We also detected CO and NO products, again finding that the CO and NO signals (due to HCNO photolysis and subsequent secondary chemistry) do not increase when H_2S is included. This fact, along with consideration of reactions 5a and 3, implies that no significant amounts of CO molecules or OH or CN radicals are produced in reaction 7. These experiments do not allow us to quantitatively measure the rate of reaction 7, but they do strongly suggest that this reaction is too slow to have a significant effect on our photolysis product detection experiments.

4. CONCLUSIONS

Infrared diode laser spectroscopy was used to study the photolysis products of fulminic acid (HCNO). The results show that five product channels have a measurable yield, and that O + HCN (1a) is the major but not dominant product channel. Photolysis quantum yields are ϕ_{1a} (O + HCN) = 0.39 ± 0.07, ϕ_{1b} (H + (NCO)) = 0.21 ± 0.04, ϕ_{1c} (CN + OH) = 0.16 ± 0.04, ϕ_{1d} (CN + NH($a^1\Delta$)) = 0.19 ± 0.03, and ϕ_{1e} (HNCO) = 0.05 ± 0.02.

AUTHOR INFORMATION

Corresponding Author

*E-mail: john.hershberger@ndsu.edu. FAX: (701)-231-8831.

Notes

The authors declare no competing financial interest.

ACKNOWLEDGMENTS

This work was supported by Division of Chemical Sciences, Office of Basic Energy Sciences of the Department of Energy, Grant DE-FG03-96ER14645.

REFERENCES

(1) Miller, J. A.; Klippenstein, S. J.; Glarborg, P. A kinetic Issue in Reburning: The Fate of HCNO. *Combust. Flame* **2003**, *135*, 357−362.
(2) Zhang, W. C.; Du, B. N.; Feng, C. J. Theoretical Investigation of Reaction Mechanism for $CH_2(X\ ^3B_1)$ with NO Radical. *J. Mol. Struct. (THEOCHEM)* **2004**, *679*, 121−125.
(3) Eshchenko, G.; Kocher, T.; Kerst, C.; Temps, F. Formation of HCNO and HCN in the 193 nm Photolysis of H_2CCO in the Presence of NO. *Chem. Phys. Lett.* **2002**, *356*, 181−187.
(4) Bauerle, S.; Klatt, M.; Wagner, H.Gg. Investigation of the Reaction of $^3CH_2$ with NO at High Temperatures. *Ber. Bunsen-Ges. Phys. Chem.* **1995**, *99*, 97−104.
(5) Grussdorf, J.; Temps, F.; Wagner, H.Gg. An FTIR Study of the Products of the Reaction between CH_2 ($X\ ^3B_1$) and NO. *Ber. Bunsen-Ges. Phys. Chem.* **1997**, *101*, 134−138.
(6) Meyer, J. P.; Hershberger, J. F. Product Channels of the HCCO + NO Reaction. *J. Phys. Chem. B* **2005**, *109*, 8363−8366.
(7) Vereecken, L.; Sumathy, R.; Carl, S. A.; Peeters, J. NOx Reduction by Reburning: Theoretical Study of the Branching Ratio of the HCCO+NO Reaction. *Chem. Phys. Lett.* **2001**, *344*, 400−406.
(8) Tokmakov, I. V.; Moskaleva, L. V.; Paschenko, D. V.; Lin, M. C. Computational Study of the HCCO + NO Reaction: Ab Initio MO/vRRKM Calculations of the Total Rate Constant and Product Branching Ratios. *J. Phys. Chem. A* **2003**, *107*, 1066−1076.
(9) Rim, K. T.; Hershberger, J. F. Product Branching Ratio of the HCCO + NO Reaction. *J. Phys. Chem. A* **2000**, *104*, 293−296.
(10) Eickhoff, U.; Temps, F. FTIR Study of the Products of the Reaction between HCCO and NO. *Phys. Chem. Chem. Phys.* **1999**, *1*, 243−251.
(11) Feng, W.; Meyer, J. P.; Hershberger, J. F. Kinetics of OH + HCNO Reaction. *J. Phys. Chem. A* **2006**, *110*, 4458−4464.
(12) Feng, W.; Hershberger, J. F. Kinetics of CN + HCNO Reaction. *J. Phys. Chem. A* **2006**, *110*, 12184−12190.
(13) Feng, W.; Hershberger, J. F. Kinetics of NCO + HCNO Reaction. *J. Phys. Chem. A.* **2007**, *111*, 3831−3835.
(14) Feng, W.; Hershberger, J. F. Kinetics of O + HCNO Reaction. *J. Phys. Chem. A* **2007**, *111*, 10654−10659.
(15) Feng, W.; Hershberger, J. F. Product Channels of the CN + HCNO Reaction. *J. Phys. Chem. A* **2012**, *116*, 10285−10292.
(16) Sheasley, W. D.; Mathews, C. W. The Ultraviolet Absorption Spectrum of HCNO in the Gas Phase. *J. Mol. Spectrosc.* **1972**, *43*, 467−471.
(17) Bondybey, V. E.; English, J. H. Infrared Spectra and Isomerization of CHNO Species in Rare Gas Matrices. *J. Mol. Spectrosc.* **1982**, *92*, 431−442.
(18) Chase, M. W. NIST-JANAF Thermochemical Tables, 4th ed. *J. Phys. Chem. Ref. Data*, **1998**, Monograph 9.
(19) Schuurman, M. S.; Muir, S. R.; Allen, W. D.; Schaefer, H. F., III. Toward Subchemical Accuracy in Computational Thermochemistry:

Focal Point Analysis of the Heat of Formation of NCO and [H,N,C,O] Isomers. *J. Chem. Phys.* **2004**, *120*, 11586−11599.
(20) Owono, L. C.; Jaidane, N.; Kwato Njock, M. G.; Ben Lakhdar, Z. Theoretical Investigation of Excited and Rydberg States of Imidogen Radical NH: Potential Energy Curves, Spectroscopic Constants, and Dipole Moment Functions. *J. Chem. Phys.* **2007**, *126*, 244302−1−13.
(21) Wilmes, R.; Winnewisser, M. Preparation of $^{15}N-^{13}C$-fulminic Acid. *J. Labelled Compd. Radiopharm.* **1993**, *33*, 157−159.
(22) Pasinszki, T.; Kishimoto, N.; Ohno, K. Two-Dimensional Penning Ionization Electron Spectroscopy of NNO, HCNO, and HNNN: Electronic Structure and the Interaction Potential with He*(2^3S) Metastable and Li(2^2S) Ground State Atoms. *J. Phys. Chem. A* **1999**, *103*, 6746−6756.
(23) Wentrup, C.; Gerecht, B.; Briehl, H. A New Synthesis of Fulminic Acid. *Angew. Chem., Int. Ed. Engl.* **1979**, *18*, 467−468.
(24) Ferretti, E. L.; Rao, K. N. Infrared Bands of the HCNO Molecule. *J. Mol. Spectrosc.* **1974**, *51*, 97−106.
(25) Steiner, D. A.; Polo, S. R.; M., T. K., Jr. Infrared Spectrrum of Fundamental ν_2 of Isocyanic Acid. *J. Mol. Spectrosc.* **1983**, *98*, 453−483.
(26) Lowenthal, M. S.; Khanna, R. K.; Moore, Marla H. Infrared Spectrum of Solid Isocyanic Acid (HNCO): Vibrational Assignments and Integrated Band Intensities. *Spectrochim. Acta, Part A* **2002**, *58*, 73−78.
(27) Rothman, L. S.; et al. The HITRAN molecular database: Editions of 1991 and 1992. *J. Quant. Spectrosc. Radiat. Transfer* **1992**, *48*, 469−507.
(28) Möllmanna, E.; Makib, M.; Winnewissera, A. G.; Winnewissera, B. P.; Quappc, W. High-Temperature Infrared Emission Spectra of $D^{12}C^{14}N$ and $D^{13}C^{14}N$. *J. Mol. Spectrosc.* **2002**, *212*, 22−31.
(29) Brüggemann, R.; Petri, M.; Fishcer, H.; Mauer, D.; Reinert, D.; Urban, W. Computer Controlled Diode Laser Spectrometer With a Helium Evaporation Cryostat and Spectroscopy of the ν_3 Vibration Of NCO. *Apply. Phys. B* **1989**, *48*, 105−110.
(30) Bernath, P. F.; Amano, T. Difference Frequency Laser Spectroscopy of the $\nu = 1\leftarrow0$ Transition of NH. *J. Mol. Spectrosc.* **1982**, *95*, 359−364.
(31) Cooper, W. F.; Hershberger, J. F. Measurement of Product Branching Ratios of the NCO + NO Reaction. *J. Phys. Chem.* **1992**, *96*, 771−775.
(32) Cooper, W. F.; Park, J.; Hershberger, J. F. Product Channel Dynamics of the NCO + NO Reaction. *J. Phys. Chem.* **1993**, *97*, 3283−3290.
(33) Geiger, H.; Wiesen, P.; Becker, K. H. A Product Study of the Reaction of CH Radicals with Nitric Oxide at 298 K. *Phys. Chem. Chem. Phys.* **1999**, *1*, 5601−5606.
(34) Sims, I. R.; Queffelec, J. L.; Defrance, A.; Rebrion-Rowe, C.; Travers, D.; Bocherel, P.; Rowe, B. R.; Smith, I. W. M. Ultralow Temperature Kinetics of Neutral−Neutral Reactions. The Technique and Results for the Reactions $CN+O_2$ Down to 13 K and $CN+NH_3$ Down to 25 K. *J. Chem. Phys.* **19994**, *100*, 4229−4241.
(35) Feng, W.; Hershberger, J. F. Reinvestigation of the Branching Ratio of the CN + O_2 Reaction. *J. Phys. Chem. A* **2009**, *113*, 3523−3527.
(36) Hack, W.; Wilms, A. Elementary reactions of imidogen ($a^1\Delta$) with atoms and diatomic molecules. *J. Phys. Chem.* **1989**, *93*, 3540−3546.
(37) Nelson, H. H.; McDonald, J. R.; Alexander, M. H. Temperature dependence of the collisional quenching of imidogen ($a^1\Delta$) by nitrogen, oxygen, carbon monoxide, and xenon. *J. Phys. Chem.* **1990**, *94*, 3291−3294.
(38) Gericke, K.-H.; Lock, M.; Comes, F. J. Photodissociation of HN_3: direct formation of hydrogen atoms. *Chem. Phys. Lett.* **1991**, *186*, 427−430.
(39) Wang, S.; Yu, J.-K.; Ding, D.-J. Theoretical study on the mechanism of OH + HCNO reaction. *Theor. Chem. ACC.* **2007**, *118*, 337−345.
(40) Zhang, W.; Du, B.; Feng, C. Theoretical study of reaction mechanism for NCO + HCNO. *Chem. Phys. Lett.* **2007**, *442*, 1−6.
(41) Li, B.; Zhang, J.; Wu, H.; Sun, G.-D. Theoretical study on the mechanism of the NCO + HCNO reaction. *J. Phys. Chem. A* **2007**, *111*, 7211−7217.
(42) Feng, W.; Hershberger, J. F. Theoretical study of the O(^{3}P) + HCNO reaction. *Chem. Phys. Lett.* **2008**, *457*, 307−311.
(43) Pang, J.-L.; Xie, H.-B.; Zhang, S.-W.; Ding, Y.-H.; Tang, A.-Q. Theoretical Study on Reaction Mechanism of Fulminic Acid HCNO with CN Radical. *J. Phys. Chem. A* **2008**, *112*, 5251−5257.
(44) Xin, Y.-N.; Zhao, M.; Li, Z.-S.; Xiong, W.; Song, X.; Hou, H.; Wang, B. Theoretical Investigation of the Reaction of Imidogen with Fulminic Acid. *J. Chem. Theory. Comput.* **2009**, *5*, 2021−2029.
(45) Wang, S.; Yu, J.; Ding, D.; Sun, J. Theoretical Study of Potential Energy Surface for the Reaction H + HCNO. *Gaodeng Xuexiao Huaxue Xuebao* **2008**, *29*, 365−368.
(46) Sander, S. P.; Abbatt, J.; Barker, J. R.; Burkholder, J. B.; Friedl, R. R;. Golden, D. M.; Huie, R. E.; Kolb, C. E.; Kurylo, M. J.; Moortgat, G. K.; Orkin, V. L.; Wine, P. H. Chemical Kinetics and Photochemical Data for Use in Atmospheric Studies, Evaluation No. 17. *JPL Publication 10−6*; Jet Propulsion Laboratory: Pasadena, CA, 2011.